SAND2022-4080C

The Role of Bipolar Amplification in the SET Response of Narrowband RF Amplifiers Using SOI CMOS

Jeffrey W. Teng, Brett L. Ringel, Justin P. Heimerl, George N. Tzintzarov, Adrian Ildefonso, Ani Khachatrian, Dale McMorrow, Phil Oldiges, and John D. Cressler

Student Paper

Abstract: Pulsed-laser measurements and circuit simulations are used to examine the role of bipolar amplification in the SET response of tuned RF amplifiers implemented in SOI CMOS. The application of body-contacting for transient mitigation is assessed.

Session Preference: Single Event Effects: Devices and ICs

Presentation Preference: Oral

Acknowledgement
This work was supported by Sandia National Laboratories.
Sandia National Laboratories is a multi-mission laboratory managed and operated by National Technology and Engineering Solutions of Sandia, LLC, a wholly owned subsidiary of Honeywell International Inc., for the U.S. Department of Energy's National Nuclear Security Administration under contract DE-NA0003525.
This paper describes objective technical results and analysis. Any subjective views or opinions that might be expressed in the paper do not necessarily represent the views of the U.S. Department of Energy or the United States Government.

Device samples were obtained through GlobalFoundries multi-project wafer runs. The authors thank N. Cahoun, A. Darbar, D. Eades, and A. Joseph of GlobalFoundries for fabrication support.

Corresponding Author:
Jeffrey W. Teng
School of Electrical and Computer Engineering, Georgia Institute of Technology,
777 Atlantic Drive NW, Atlanta, GA 30332-0250 USA
USA Phone: 262-893-0223
Email: jteng9@gatech.edu

Contributing Authors:
Brett L. Ringel, Justin P. Heimerl, George N. Tzintzarov
John D. Cressler
School of Electrical and Computer Engineering, Georgia Institute of Technology, Atlanta, GA 30332 USA

Adrian Ildefonso, Ani Khachatrian, Dale McMorrow
U.S. Naval Research Laboratory, Washington, DC 20375 USA

Phil Oldiges
Sandia National Laboratories, Albuquerque, NM 87185 USA

I. Introduction

Silicon-on-insulator (SOI) CMOS transistors are commonplace in high-density, high-speed, and low-power digital circuits. By placing CMOS transistors on an isolating buried oxide (BOX), parasitic capacitances to the silicon substrate are eliminated, improving circuit speed. However, by doing so, a bipolar amplification phenomenon occurs [1]–[5]. When ionizing particles generate single-event transients (SETs) in floating-body (FB) transistors, carriers trapped in their bodies “turn-on” the parasitic *npn* bipolar junction transistor (BJT) formed by the source (n-type), body (p-type), and drain (n-type), resulting in a dramatic extension of the duration of SETs after a particle strike. This extended duration leads to system-level concerns for communications systems. For example, “tuned” amplifiers are often found in the front-ends of communications receivers. To increase the signal amplitude and reject out-of-band noise, these amplifiers are designed to operate across a narrow range of frequency. A long-duration SET in such an amplifier may corrupt the data stream across multiple bits. Thus, a method to reduce the transient duration in tuned RF amplifiers is desirable.

A known method to mitigate the bipolar-amplification tail is to add grounded body contacts to sensitive transistors [5], [6]. In this case, the holes that are typically trapped in floating bodies of SOI devices are extracted through the body contact, preventing a long transient duration [7]. For digital circuits (e.g., memory), this mitigation technique can reduce single-event upset (SEU) cross-sections by reducing the probability of collected charge (CC) exceeding the critical charge for bit flips during transient events [3], [6], [8], [9]. For RF circuits, however, CC is not necessarily a good metric for SET sensitivity. While the load of a digital circuit is primarily capacitive, the load of an RF circuit is primarily resistive at the frequency of operation. Further, for RF circuits, adding body contacts comes at a cost in performance. The addition of body contacts returns a portion of the capacitance that was removed by using SOI, degrading noise, gain, and bandwidth [10]. This tradeoff of performance must be considered as well as any potential benefit in the SET response.

In the present work, the role of bipolar amplification in the SET response of tuned RF amplifiers is examined in order to support the potential use of SOI CMOS in next-generation space-borne communications systems. Two-photon absorption (TPA) induced by laser pulses was used to collect transients in both nMOS devices and a K_u-band low-noise amplifier (LNA), thereby informing TCAD and circuit simulations to understand how transients with bipolar amplification tails propagate in tuned RF amplifiers. Finally, the tradeoff between transient sensitivity and LNA performance due to the use of body-contacting is discussed. The results of the present work demonstrate that body-contacting incurs significant RF performance degradation, with minimal benefit to the SET response.

II. nMOS Experiment

SOI CMOS transistors were taken from GlobalFoundries 45-nm RFSOI technology process technology [11]. nMOS transistors with gate length of 45 nm, finger width of 1 μm, and 20 fingers were tested with bodies floating. The SOI which forms the bodies of the nMOS is partially depleted in this technology platform.

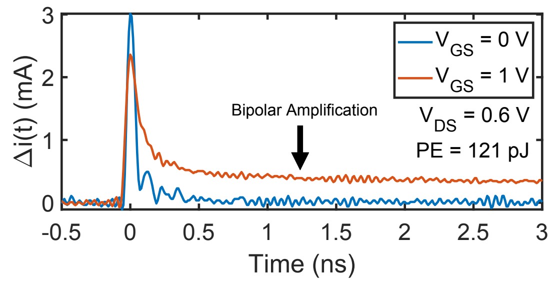

Fig. 1. Comparison of source transients at V_{GS} = 0 V and 1 V with the same V_{DS}. The extended tail due to bipolar amplification is indicated with an arrow.

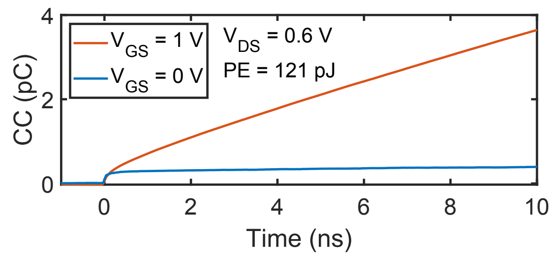

Fig. 2. Comparison of collected charge (CC) at V_{GS} = 0 V and 1 V with the same V_{DS}. Note the difference in time scale compared to Fig. 1.

To collect SET data, charge was deposited in these nMOS transistors through the backside of the silicon die using TPA induced by laser pulses. The laser pulses were generated at the U.S. Naval Research Laboratory by an optical parametric amplifier pumped by a Clark-MXR CPA2110 Ti:Sapphire system. The pulses were centered at a wavelength of 1260 nm, with a pulse width of 150 fs, a repetition rate of 1 kHz, and a focused spot size of 1.3 μm full-width-at-half-maximum. A pulse energy (PE) of 121 pJ was used. Three 1-dimensional raster scans were performed to center the laser spot over the transistor, which was identified as the location with the maximum transient amplitude. Resulting current transients, $\Delta i(t)$, were collected using a Textronix MSO72004C mixed-signal oscilloscope with analog bandwidth of 20 GHz and sample rate of 100 GS/s. Anritsu K251 bias tees were used, and gate-source voltage (V_{GS}) and drain-source voltage (V_{DS}) were provided by Keithley 2400 SourceMeters.

Because these RF-optimized transistors have high gain, parasitic oscillations can occur due to RF instability, which obscure transient measurements. To avoid this problem, the transistors were measured in common-drain (CD) configuration (drain grounded), wherein the device exhibits improved RF stability. All data presented in the present work uses the CD configuration. Where possible, common-source (CS) transients were also recorded for comparison. Drain and source transients were observed to be equal but opposite in sign, as expected. The equivalence of source and drain transients was also reported in [12] for some bias conditions.

A. nMOS Results

Measured source transients are shown in Fig. 1. When V_{GS} is low, the parasitic BJT is weakened, and the long transient tail is less apparent. Then, when V_{GS} is set high to turn on

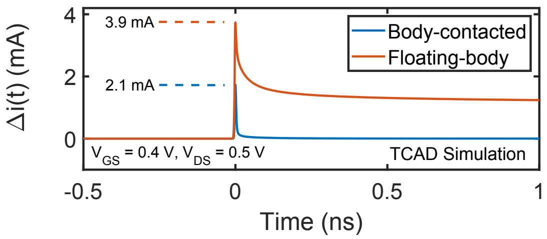

Fig. 3. TCAD device transients with and without body contacting, demonstrating a reduction in both transient amplitude and duration.

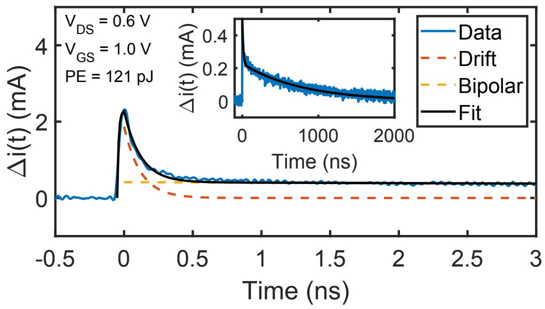

Fig. 4. Example source transient at V_{DS} = V_{GS} = 0.6 V and pulse energy of 121 pJ. A fit line is superimposed, with drift-diffusion (I_{dd0}, τ_{dd}) = (3.46 mA, 69.7 ps) and bipolar amplification (I_{npn0}, τ_{npn}) = (0.507 mA, 173 ns) components decomposed. The inset shows a longer capture duration to highlight the bipolar amplification tail.

the nMOS transistor, the parasitic BJT is fully turned on. For the time scale in Fig. 1, the bipolar-amplification tail at high V_{GS} appears as a plateau of current.

The increase in CC during this extended transient tail may impact some digital circuits. In logic circuits, the load impedance is primarily capacitive, which effectively integrates the transient current, yielding a charge. Hence, the critical charge is the CC at which a transient causes a logic circuit to switch states. Fig. 2 shows the increase in CC due to bipolar amplification. Even after 10 ns, the CC still has not settled for the case with bipolar amplification operative. For some types of digital circuits the extension of the transient duration due to bipolar amplification can lead to a larger SEU cross-section [5], [6].

To evaluate the effects of body contacts on the device transient, Sentaurus TCAD [13] was used to simulate transient events, both with and without grounded body contacts. Devices were modeled in 2 dimensions, and a charge track with 0.1 pC/μm was used. Full details of the TCAD and validation of TCAD results using comparisons with measurements will be added to the full paper. Simulated transients are shown in Fig. 3. The bias condition was chosen to represent the LNA test conditions below. By connecting the body to an ideal ground, the bipolar amplification tail is eliminated. At the same time, some of the deposited charge is drawn out of the body contact, so the transient amplitude at the source/drain is reduced by about 50%, consistent with measurements by England *et al.* [3]. The reductions in both amplitude and duration translate to lower CC, illustrating the benefits of body contacting reducing CC.

B. Circuit-level Transient Modeling

To understand how a device SET propagates within a circuit, the device-level transient was modeled with an analytical expression. The SET is decomposed into two components. Initially, deposited electrons are rapidly swept away by the fields inside the device, causing an initial fast peak. This fast part is the drift-diffusion component. Then, holes trapped in the floating body lead to bipolar amplification, which manifests as a long tail lasting multiple μs [1], [2].

TABLE I
K_u-BAND LNA PERFORMANCE

Parameter	FB	BC
Bandwidth (GHz)	12.5 – 16	13.5 – 15.5
Return Loss (dB)	10	10
Gain (dB)	16.5	15.3
Noise Figure (dB)	1.0	1.7
Supply Voltage (V)	1.0	1.0
Supply Current (mA)	8.3	8.0

In order to model this transient waveform in a circuit simulation, a fit function inspired by Black *et al.* [14] was utilized. This previous work focused on inverter cells in a bulk process, which are modeled by a “dual-double-exponential” form. The present work simplifies that model to remove components not necessary for single transistors. To capture both the initial peak and bipolar amplification tail, the sum of two exponentials is used, following an exponential rise:

$$\Delta i(t) = \begin{cases} 0 & t < -5\tau_r \\ (I_{dd0} + I_{npn0})\left[1 - e^{-(t+5\tau_r)/\tau_r}\right] & -5\tau_r \leq t < 0 \\ I_{dd0}e^{-t/\tau_{dd}} + I_{npn0}e^{-t/\tau_{npn}} & t > 0 \end{cases} \quad (1)$$

I_{dd0} is the amplitude of the initial drift-diffusion component, with time constant τ_{dd}, and I_{npn0} is the amplitude of the bipolar amplification tail, with time constant τ_{npn}. To fit the rising edge, τ_r is the rising time constant. Curve fitting for all five parameters was performed using nonlinear least-squares regression in MATLAB [15]. A comparison of the fit with the measured transient in Fig. 4 shows excellent agreement.

Bipolar amplification has been shown to be dependent on the transistor bias condition, which in turn controls the current gain of the parasitic BJT. Thus, another method in which to control bipolar amplification is to adjust the transistor bias conditions during the design of an amplifier. To examine this potential trade space in addition to body contacting, SETs were also collected across V_{DS} and V_{GS}. Fitting of transients according to (1) was performed at each bias condition.

The extracted transient amplitudes ($I_{dd0} + I_{npn0}$) are shown in Fig. 5, for various device biases. Corresponding τ_{dd} and τ_{npn} are shown in Fig. 6 and Fig. 7, respectively. Raising V_{DS} increases the transient amplitude while reducing both τ_{dd} and τ_{npn} in most cases. Meanwhile, raising V_{GS} decreases the amplitude and simultaneously decreases τ_{npn}, which dominates the overall transient duration. For circuit designs targeting applications subject to transient radiation effects, amplitude and duration of transients can be considered when selecting device biases, in addition to electrical performance. The data in Figs. 5–7 are used to examine the LNA’s SET response in multiple bias configurations below.

III. KU-BAND LNA EXPERIMENT

To evaluate the effectiveness of body contacting in RF circuits, a K_u-band LNA was designed and fabricated in the same 45-nm SOI CMOS technology platform as transistors

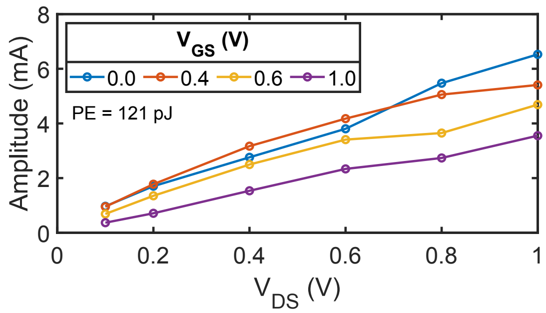

Fig. 5. Source transient amplitude as a function of V_{DS} for various V_{GS} at a fixed pulse energy of 121 pJ.

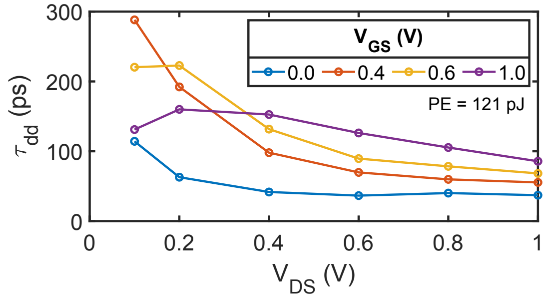

Fig. 6. τ_{dd}, extracted from measurement results, as a function of V_{DS} for various V_{GS} at a fixed pulse energy of 121 pJ.

tested above. The device sizes were intentionally chosen to match those tested above. The schematic of this LNA is shown in Fig. 8, and its performance is given in Table I. The tested LNA used FB devices to maximize performance. Another LNA with identical device sizes and passive components was also simulated, but with body-contacted (BC) devices (bodies grounded) instead of FB devices. Observe that the LNA with BC devices exhibits degradation in bandwidth, gain, and noise figure compared to the FB LNA due to the additional parasitic capacitances mentioned above [10]. Given this cost of performance, the efficacy of body contacting to mitigate SETs must be carefully explored.

The same oscilloscope and power supplies used for transistor testing were used to characterize the LNA. The gate bias voltage, V_{GG}, was supplied from off-chip using a bias tee. Transient data was collected for laser pulses over the CS device of the cascode LNA. Previous testing has demonstrated that the function of the CS device as a current source for the common-gate (CG) device inhibits the transient when the CG device is struck [3], [16]. Thus, the present work focused on the CS device.

In addition to the measured results, circuit-level simulations were also used to investigate the propagation of device transients in the LNA. SETs were simulated by injecting a current source between the drain and source of the struck CS device. $\Delta i(t)$ is of the form in (1). To model the measurement setup, 500-pH inductors were added to both the input and output in simulation, which represent wirebonds that connected the LNA to the test board [17]. The Anritsu bias tees were modeled using a 1-mH inductor and 20-pF capacitor. The oscilloscope input was modeled as a 300-fF capacitor in parallel with a 50-Ω termination. Transient simulations were performed in Cadence Spectre [18], which uses the forward-Euler method. Transient model parameters

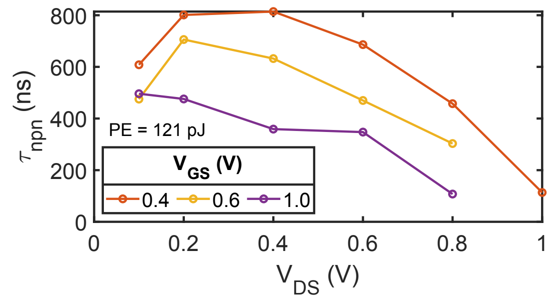

Fig. 7. τ_{npn}, extracted from measurement results, as a function of V_{DS} for various V_{GS} at a fixed pulse energy of 121 pJ. V_{GS} of 0 V is not shown, since the second time constant was not necessary to fit the measured transients.

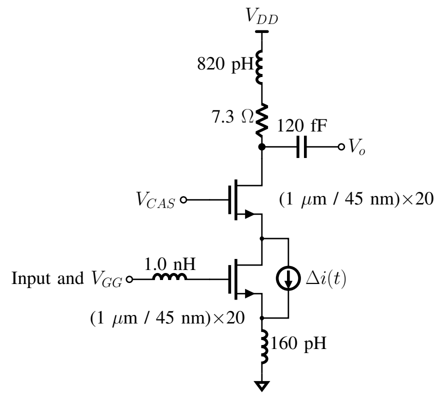

Fig. 8. Schematic of the tested K_u-band LNA. Gate bias V_{GG} was supplied through a bias tee in measurement. The current source across the bottom transistor was used to model an SET in circuit simulation.

were selected according to the simulated quiescent operating point of the target device.

A. LNA Results

A comparison of measured and simulated transients is provided in Fig. 9. The simulated result matches the measured data well enough to give qualitative insights into the LNA's transient response. Measurement and simulation also agreed at various biases of the LNA, but is not shown, for brevity.

To investigate how bias might be used to mitigate the transient, simulated LNA output transients and their corresponding $\Delta i(t)$ are shown for two bias conditions in Fig. 10. The top pane shows a case where for low V_{GS} compared to the nominal bias in the bottom pane. When the amplitude of the device transient is larger, the LNA output amplitude is correspondingly larger. However, note that when V_{GG} is 0.4 V, even though the bipolar amplification tail is present, the effective duration of the LNA output transient is shorter than when V_{GG} is 0.2 V. Accordingly, bias conditions may be used to adjust amplitude, but the duration of the LNA transient is not directly related to the duration of the device transient. In fact, V_{GG} of 0.2 V gives lower gain than 0.4 V, so this example demonstrates the possibility to simultaneously reduce SET amplitude and improve RF performance at the cost of power consumption by raising V_{GG}.

To explain further, note that the load of the LNA includes an inductor, which is a short-circuit at low frequencies. Further, note that $1/\tau_{npn}$ in Fig. 7 is on the order of 10 MHz, far below the bandwidth of the tested LNA, which operates from 12.5–16 GHz. Accordingly, the current due to the bipolar amplification tail passes through the load inductor to V_{DD}

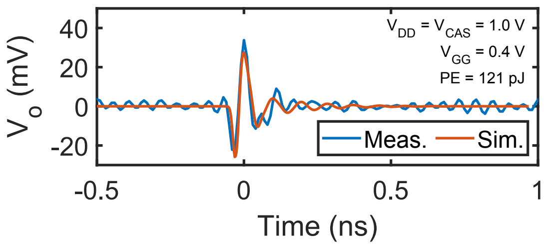

Fig. 9. Simulated LNA output waveforms for two bias conditions, illustrating the dependence of LNA amplitude and duration on device amplitude and duration. Persistent oscillations are due to noise in the measurement system.

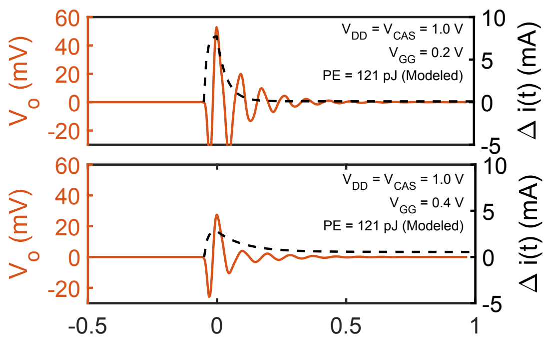

Fig. 10. The simulated LNA output transients with corresponding modeled $\Delta i(t)$ at 121 pJ overlaid for low V_{GG} (top) and nominal V_{GG} (bottom) cases. Scales are made equal for ease of comparison.

instead of reaching the output. This behavior is verified by tracking the current through the power supply and the 50-Ω termination impedance in simulation, as in Fig. 11. While the high-frequency ringing passes through the output capacitor to the load, the low-frequency bipolar amplification tail is rejected and does not contribute to the LNA output transient.

B. Body-Contacting in Tuned Amplifiers

Using the transient simulations from TCAD in Fig. 3, corresponding LNA transients were simulated and are shown in Fig. 12. The amplitude of the LNA decreased by 50% with body contacting, the same reduction as the device transient. That is, reducing the device-level transient amplitude using body contacts offers proportional improvements in amplifier-level transient amplitude. However, consider that most space applications sensitive to SETs receive signals near their minimum receiver sensitivity, typically tens of μV in amplitude. In this case, even a 50% reduction in transient amplitude thanks to body-contacting may not offer any benefit for SET mitigation in a communications receiver.

On the other hand, for any amplitude large enough to cause system-level disturbances, a long-duration transient can be especially problematic for analog/RF circuits [19]. In terms of duration, body-contacting does not offer significant improvements. Originally, the FB LNA rejected long-duration transient tails naturally, so the addition of body contacts makes little difference to the duration of the LNA transient. Unless the transient amplitude is reduced enough to become negligible for system impact, which is unlikely, adding body contacts to a tuned RF amplifier leads only to an RF performance degradation with minimal benefits for the SET response.

IV. Summary

The role of bipolar amplification in the SET response of tuned RF amplifiers implemented with SOI CMOS is investigated. Charge generated via TPA using optical laser pulses was used to induce SETs in nMOS devices and a corresponding K_u-band amplifier. Modeling and circuit simulation show that transient tails due to bipolar amplification are inherently filtered out by the nature of tuned amplifiers, which have parallel inductors in their loads. While body-contacting as a mitigation technique is effective for reducing CC, there is no significant impact on the SET duration at the LNA output from bipolar amplification tails. Thus, at the cost of RF performance degradation, body-contacting offers only minor benefits for SET amplitude with no reduction in duration.

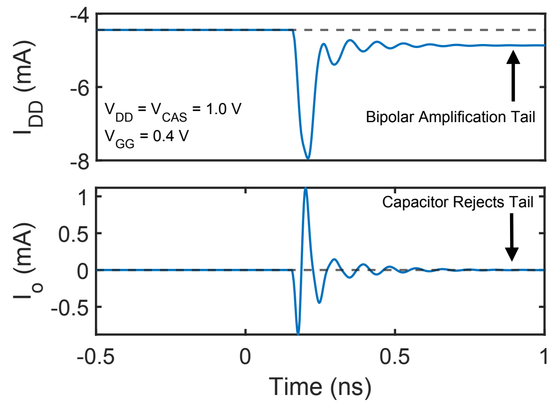

Fig. 11. The simulated current through the power supply (I_{DD}) and the 50-Ω load (I_o).

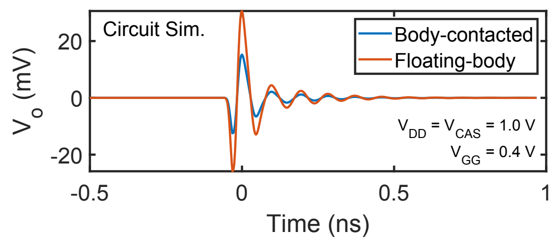

Fig. 12. Comparison of simulated LNA output transients with and without body contacting.

References

[1] L. Massengill *et al.*, *IEEE EDL*, vol. 11, no. 2, pp. 98–99, Feb. 1990.
[2] O. Musseau *et al.*, *IEEE TNS*, vol. 47, no. 6, pp. 2196–2203, Dec. 2000.
[3] T. England *et al.*, *IEEE TNS*, vol. 60, no. 6, pp. 4405–4411, Dec. 2013.
[4] T. Makino *et al.*, *IEEE TNS*, vol. 56, no. 1, pp. 202–207, Feb. 2009.
[5] V. Ferlet-Cavrois *et al.*, *IEEE TNS*, vol. 49, no. 6, pp. 2948–2956, Dec. 2002.
[6] V. Ferlet-Cavrois *et al.*, *IEEE TNS*, vol. 57, no. 4, pp. 1811–1819, Aug. 2010.
[7] K. A. Moen *et al.*, *IEEE TNS*, vol. 57, no. 6, pp. 3366–3372, Dec. 2010.
[8] J. Alvarado *et al.*, in *2009 RADECS*, Sep. 2009.
[9] P. Gouker *et al.*, *IEEE TNS*, vol. 55, no. 6, pp. 2854–2860, Dec. 2008.
[10] A. Madan *et al.*, *IEEE MWCL*, vol. 22, no. 4, pp. 200–202.
[11] S. Lee *et al.*, in *2007 IEDM*, Oct. 2007.
[12] Z. E. Fleetwood *et al.*, *IEEE TNS*, vol. 62, no. 6, pp. 2643–2649, Dec. 2015.
[13] https://www.synopsys.com/silicon/tcad.html, Accessed: April 4, 2022.
[14] D. A. Black *et al.*, *IEEE TNS*, vol. 62, no. 4, pp. 1540–1549, Aug. 2015.
[15] https://www.mathworks.com/help/optim/nonlinear-least-squares-curve-fitting.html.
[16] N. E. Lourenco *et al.*, *IEEE TNS*, vol. 63, no. 1, pp. 273–280, Feb. 2016.
[17] https://www.iee.et.tu-dresden.de/iee/eb/forsch/AK-Bipo/2014/AKB2014_04_IFX_Berkner.pdf, Accessed: April 4, 2022.
[18] https://www.cadence.com/en_US/home/tools/custom-ic-analog-rf-design/circuit-simulation/spectre-simulation-platform.html.
[19] S. E. Armstrong *et al.*, *IEEE TNS*, vol. 58, no. 3, pp. 1066–1071, Apr. 2011.